Intermittencies in complex Ginzburg–Landau equation by varying system size*

Li Hai-Hong(李海红)[a)†], Xiao Jing-Hua(肖井华)[a)b)],
Hu Gang(胡 岗)[b)c)], and Hu Bambi(胡斑比)[b)d)]

[a)] *School of Science, Beijing University of Posts and Telecommunications, Beijing* 100876, *China*
[b)] *Centre of Nonlinear Studies and Department of Physics, Hong Kong Baptist University, Hong Kong, China*
[c)] *Department of Physics, University of Houston, Houston, TX* 77204, *USA*
[d)] *Department of Physics, Beijing Normal University, Beijing* 100875, *China*

(Received 6 July 2009; revised manuscript received 26 October 2009)

The dynamical behaviour of the one-dimensional complex Ginzburg–Landau equation (CGLE) with finite system size L is investigated, based on numerical simulations. By varying the system size and keeping other system parameters in the defect turbulence region (defect turbulence in large L limit), a number of intermittencies new for the CGLE system are observed in the processes of pattern formations and transitions while the system dynamics varies from a homogeneous periodic oscillation to strong defect turbulence.

Keywords: Ginzburg–Landau equation, chaos, turbulence
PACC: 0547, 9210L, 6120J

1. Introduction

Over many decades the problem of pattern formation in spatiotemporal systems has attracted long standing interest.[1−17] Recently, a focus in this direction has gone to the topic of transitions from low-dimensional regular or chaotic patterns to high-dimensional spatiotemporal chaos or turbulence. Usually, for a small system size (say, L), an extended system has a low-dimensional state, either regular (periodic or quasi-periodic) or chaotic, since only a small number of modes can be activated then. By increasing L the system may reach a high-dimensional fully-developed turbulent state for sufficiently large L. Therefore, by changing the system size, one can build up an ideal bridge, linking both low- and high-dimensional sides and exploring the rich dynamic behaviour in between.

In the past, for studying spatiotemporal chaos and turbulence, the majority of works have considered a large system size limit, and the influence of the system size has been ignored.[6,8−10] As new techniques develop so quickly, scientists can now easily produce very small devices and can control various system parameters, including the boundary conditions. Thus, the road from low-dimensional state to high-dimensional turbulence by varying the system size can be manifested in great detail, and the rich behaviour in this transition can be observed by experiments and possibly utilised in practical applications.

With increasing system size L, rich bifurcations and associated pattern formations and spatial symmetry variations can be observed accompanying the tendency of more chaotic temporal behaviour and symmetry reducing and breaking. Intermittency, which was observed in many real and numerical models, has recently become an important research topic.[18−20] In this study, we will focus on some intermittencies new observed in the process of complicated transitions between different pattern formations. Specifically, we consider the following one-dimensional (1D) complex Ginzburg–Landau equation (CGLE)[5−9]

$$\partial_t A = A + (1 + \mathrm{i}c_1)\frac{\partial^2 A}{\partial x^2} + (1 + \mathrm{i}c_2)\,|A|^2 A, \qquad (1)$$

with periodic boundary condition of length L

$$A(x + L, t) = A(x, t). \qquad (2)$$

*Project supported by grants from the Hong Kong Research Grants Council (RGC) and Hong Kong Baptist University Faculty Research Grants (FRG), and partially supported by the National Natural Science Foundation of China (Grant No. 10575016) and Nonlinear Science Project of China.
†Corresponding author. E-mail: haihonglee@gmail.com
© 2010 Chinese Physical Society and IOP Publishing Ltd

Equation (1) can be generally derived, as the universal form, from a spatiotemporal system slightly beyond a homogeneous Hopf bifurcation point, where $A(x,t)$ is the order parameter. This equation has been extensively investigated for the pattern formation and turbulence problems. It is well known that the CGLE has the following plane wave solutions

$$\begin{aligned} &A(x,t) = A_0\,\mathrm{e}^{\mathrm{i}(qx-\omega_q t)},\\ &A_0 = \sqrt{1-q^2}, |q|<1,\\ &\omega_q = c_2 + (c_1-c_2)q^2. \end{aligned} \tag{3}$$

In the limit $L\to\infty$ there exists a BF instability[21] line $1+c_1c_2=0$, beyond which $(1+c_1c_2<0)$ all the plane wave solutions (3) become unstable, and the system turns to be chaotic. The chaotic state can be classified to phase turbulence or defect turbulence states in different parameter regions.[9,10] So far, most of works have considered the large system size limit, then the transition from the periodic plan wave to the chaotic state occurs sharply on a BF curve. Moreover, the transitions between different turbulent states are ambiguous in some sense.

The system size L in Eq. (1) is a relevant parameter in the equation. For instance, with a finite system size the BF curve may develop to a bifurcation zone in the (c_1,c_2) plane with certain width. It is interesting to explore the fine structure in this zone. Alternatively, we can also fix c_1,c_2 parameters in a certain turbulence region, and study this zone structure by varying the system size. In this study, we fix $c_1=2.1, c_2=-1.5$, to make the system deeply in the fully-developed defect turbulence region for $L\to\infty$ and examine the system behaviour for different sizes L.

In this study, three different new intermittencies are investigated when the CGLE system transits from a homogeneous periodic state to a violent turbulent state by increasing the system size. The paper will be organised as follows. In Section 2, we will compute Lyapunov exponents of the systems, then different kinds of motions (periodic, quasiperiodic, or chaotic), appearing by varying the system size L, can be clearly identified. In Section 3, three types of intermittencies new for the CGLE system are found when the CGLE is adjusted from regular states to chaotic ones. The Section 4 is devoted to a discussion on the general picture of the road from low-dimensional state to high-dimensional turbulence and the important roles of these new intermittencies on the transition process of pattern formations by increasing the system size. The main body of the paper presents numerical observations, but an effort on intuitively understanding some interesting features can be also apparently seen in the work. For numerical computation the pseudospectral integration method is applied throughout the paper, and the validity of the numerical results is checked by reducing the space and time steps.

2. Lyapunov exponents and spatial patterns for various system sizes L

First, we consider two limit cases of small and large Ls. For very small L, the system must take a stable homogeneous periodic (HP) solution

$$\begin{aligned} &\widehat{A}(x,t) = A_0\,\mathrm{e}^{\mathrm{i}\omega t},\\ &A_0 = 1, \quad \omega = c_2, \end{aligned} \tag{4}$$

due to the diffusion term in Eq. (1). For sufficiently large L, the system must be chaotic for both time and space, since the parameters c_1 and c_2 are taken in the defect turbulence region. The time sequence at a single space point and the spatiotemporal pattern are shown in Figs. 1(a) and 1(b) for $L=6.5$ (small L), and in Figs. 1(c) and 1(d) for $L=24$ (large L) respectively.

The main interest of this work is on the system behaviour for intermediate L. We can start our investigation with the stability analysis of the solution (4). Inserting $\Delta A = A(x,t)-\widehat{A}(x,t) = \delta\,\mathrm{e}^{\mathrm{i}kx+\sigma t}$ into Eq. (1) and keeping only the linear terms of δ, the eigenvalue σ can be solved as

$$\sigma = -(k^2+1) \pm \sqrt{1-c_1^2k^4-2c_1c_2k^2}. \tag{5}$$

In Fig. 2(a) we plot $\mathrm{Re}(\sigma)$ vs k, and find that $k_c\approx 0.8915$ is the critical wave number for the instability. For finite L, k can be realised only on discrete values as

$$k_n = \frac{2\pi n}{L}, \quad n=\pm1,\pm2,\ldots\ . \tag{6}$$

In Fig. 2(b) we plot the k_n-L curves, and the system lengths for the instabilities of different modes are identified by the crossings of these curves with the horizontal line, L_n. It is obvious that after $L>L_1\approx 7.04$ the simple synchronous periodic solution loses its stability due to the instability of $n=1$ mode.

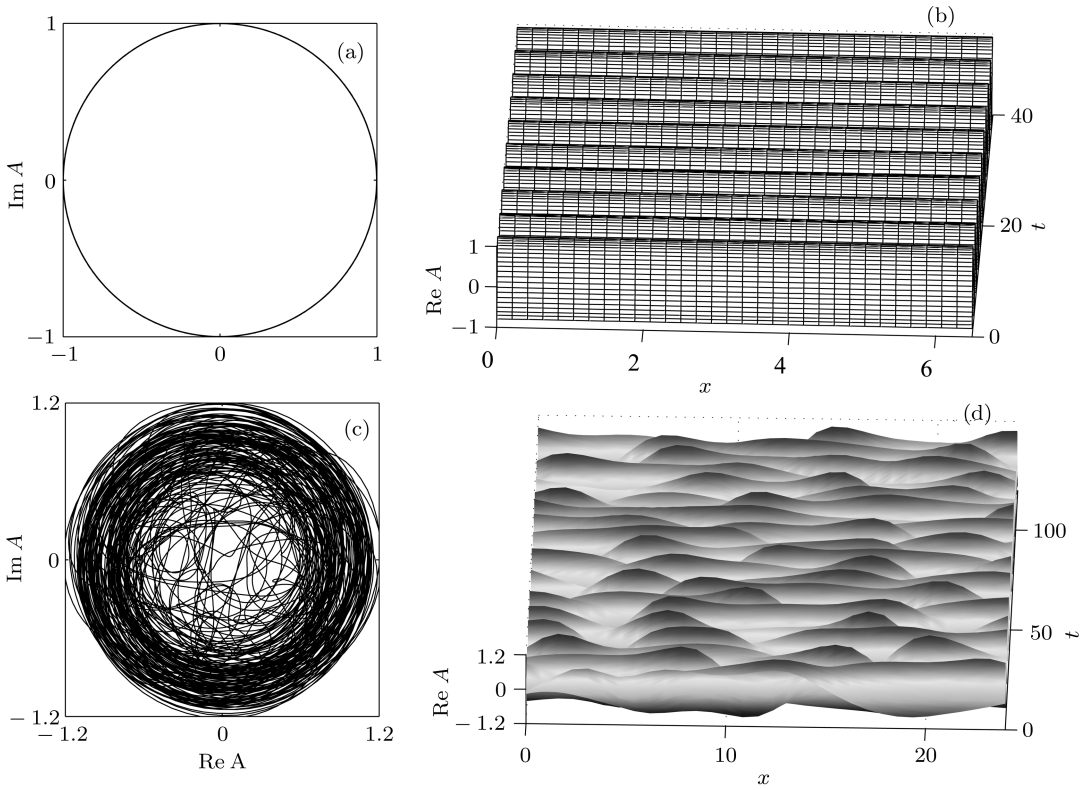


Fig. 1. Parameters $c_1 = 2.1, c_2 = -1.5$ are used in all the following figures. (a) The trajectory of $A(x,t)$ at an arbitrary space point for $L = 6.5$. The motion is periodic. (b) The spatiotemporal pattern of $\mathrm{Re}A(x,t)$ for $L = 6.5$. The state is homogeneous and periodic. (c) The same as (a) with $L = 24$. A strongly chaotic motion is observed. (d) The same as (b) with $L = 24$, spatiotemporal chaos is apparent.

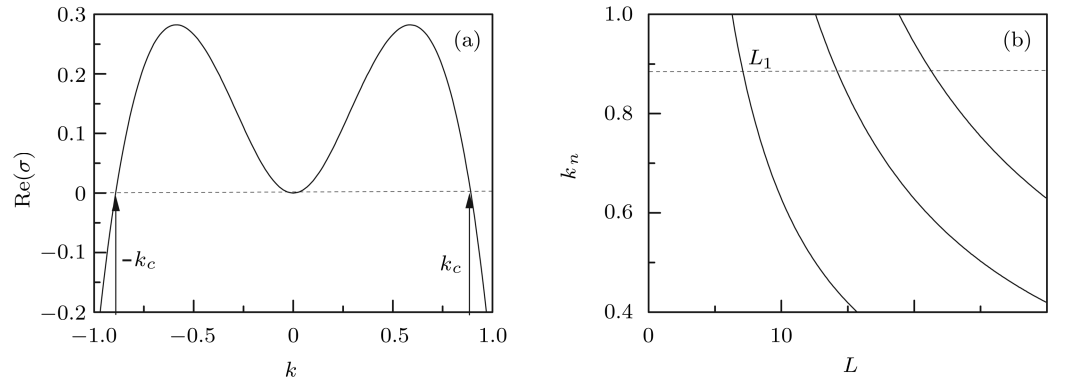


Fig. 2. (a) Re (σ) vs k in Eq. (5). Re (σ) is positive for $|k| < k_c \approx 0.8915$. The homogeneous periodic state loses its stability if any mode has wave number in this instability region. (b) $k_n(L)$ vs L. k_n is the wave number of the nth mode. At $L > L_n$ the solutions of (4) with mode-k $k \geq n$ unstable. All the solutions of (4) with $k \geq 1$ are unstable for $L > L_1 \approx 7.04$.

For having an overall view of the system behaviour for intermediate L we plot the first four Lyapunov exponents (LE) of Eq. (1) vs L in Fig. 3. It shows indeed that the homogeneous periodic solution (4) is the stable solution only for $L < L_1$, and spatiotemporal chaos dominate for $L > L_T \approx 18.746$. In the region of $L_1 < L < L_T$, rich patterns and bifurcations are observed. The abbreviated expressions in Fig. 3 have the following meanings:

HP: homogeneous periodic state; PSW: periodic standing waves in the form of $A(x,t) = A_0(x)\,\mathrm{e}^{\mathrm{i}\phi(x)}\,\mathrm{e}^{\mathrm{i}\omega t}$; Q2BW: two-frequency quasiperiodic breathing waves in the form of $A(x,t) = A_0(x,t)\,\mathrm{e}^{\mathrm{i}\phi(x,t)}\,\mathrm{e}^{\mathrm{i}\omega t}$, which has two frequencies ω and $\omega_1 = 2\pi/T$, where T is the period of phase $\phi(x,t)$; Q2RW: two-frequency quasiperiodic running wave with the form of $A(x,t) = A_0(x-vt)\,\mathrm{e}^{\mathrm{i}\phi(x-vt)}\,\mathrm{e}^{\mathrm{i}\omega t}$; Q3BW: three-frequency quasiperiodic breathing wave;

Q3RW: three-frequency quasiperiodic running wave with the form of $A(x,t) = A_0[(x-vt),t]\,\mathrm{e}^{\mathrm{i}\phi[(x-vt),t]}\,\mathrm{e}^{\mathrm{i}\omega t}$; CW: chaotic waves.

In the next section we focus on the intermittent behaviours at the transitions between the above states.

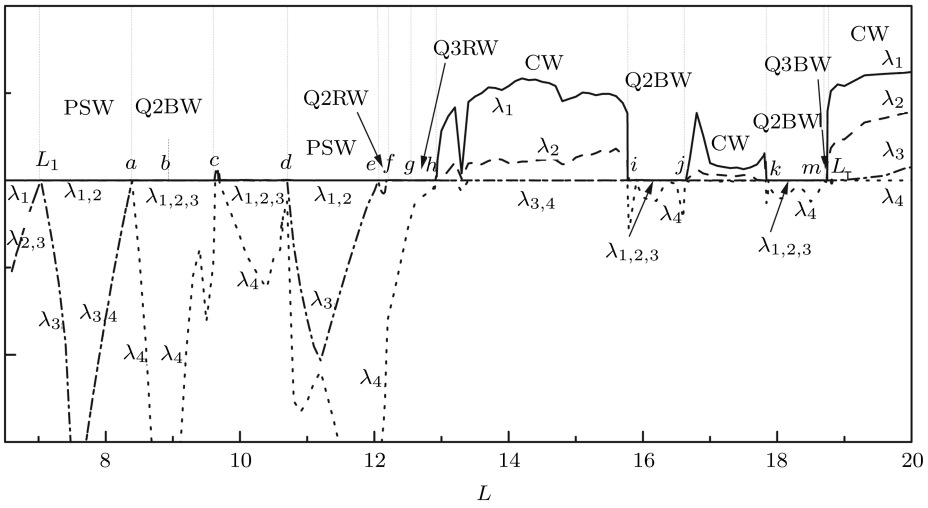


Fig. 3. The largest four LEs plotted vs L. At points $L_1, L_a, \ldots, L_T$ one can find various bifurcations. The meanings of the states HP, PSW, Q2BW, Q2RW, Q3RW, Q3BW and CW are explained in the text.

3. Intermittencies and bifurcations to homogeneous turbulence

Intermittencies are significant topic in nonlinear dynamical systems which bridge the transitions between different dynamical behaviours not only in single oscillator system but also in coupled systems. For example, intermittency is a well-known one road to chaos[22] or a road to complete synchronisation in coupled systems.[23] Moreover, intermittent behaviour is even much more interesting and richer in spatiotemporal systems since both time and space variables are involved in these processes. In our model we find a number of intermittencies new for the CGLE system in the bifurcation processes of different wave patterns by increasing system size L.

3.1. Intermittent random walk of the S_{M} axis of the Q2BW pattern at L_c

In our system the Q2BW state can be very easily observed [with the intervals of $(L_a, L_c), (L_i, L_j), (L_k, L_m)$]. All these states have, at least, a mirror symmetry (S_{M}) axis. The position of this axis is stable whenever it stands up, though different initial conditions can result in different positions of the axis due to the translational symmetry (S_{T}) of Eq. (1). Nevertheless, the stability of the axis may be lost at certain bifurcations. In Figs. 4(a) and 4(b) we show the spatiotemporal patterns around L_c. In Fig. 4(a) a Q2BW state is apparent, while in Fig. 4(b) intermittent bursts are observed in the evolution. Between any two neighbour bursts, we can find a laminar pattern which is almost the same as the Q2BW state in Fig. 4(a), however, the mirror symmetry (S_{M}) axis of the laminar state makes a random walk during each burst. After each burst, the whole pattern shifts a certain distance by keeping the same shape. The time intervals between any two bursts and the distances of the pattern shifts at different bursts are different and random. This randomness leads to a small positive λ_1 and the state is regarded as weak chaos. The positions of the points $\mathrm{d}A_0(x,t)/\mathrm{d}x = 0$ vs time t for the patterns of Figs. 4(a) and 4(b) are shown in Figs. 4(c) and 4(d), respectively. The instant symmetry axis must be located at these points. The stability of the location of the axis for $L < L_c$ (see the straight lines on $x = 0, L/2$ in Fig. 4(c)) and the intermittency of random walk of the axis for $L > L_c$ (the random moving of the two straight segments Fig. 4(d)), are clearly seen.

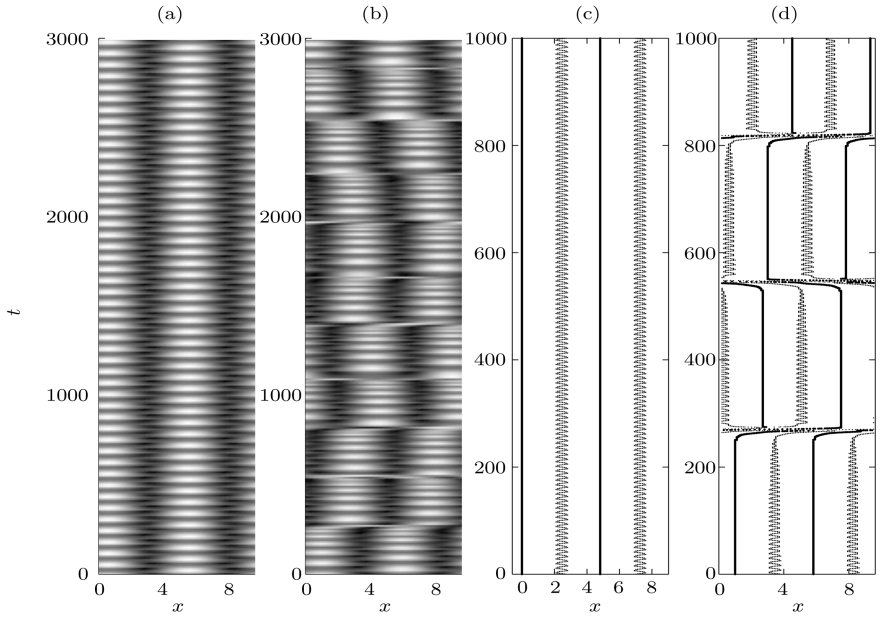


Fig. 4. The chaotic intermittency around $L_c \approx 9.626$. (a) $L = 9.625 < L_c$, the pattern of a Q2BW state. (b) $L = 9.63 > L_c$, an intermittent state, the pattern is practically the same as (a) in the laminar phase while it makes random walk during the bursts. (c), (d) The trajectories of the points $A_0(x,t)_{\max}$ for $L = 9.625$ (c) and $L = 9.63$ (d), respectively. The two straight lines in (c) represent the fixed $S_{\rm M}$ symmetry axis $(0, L/2)$. In (d) these straight segments make random walks during bursts.

For $L < L_c$, the behaviours at different space points are different in the Q2BW state since the $S_{\rm M}$ symmetry axis is fixed, then apart from the $S_{\rm M}$ symmetry pairs different points are not equivalent. However, after the intermittency, no points take particular position in the state, the statistical translational symmetry is recovered by the intermittent bursts. Let us define statistical translational symmetry such that, for any function $f(A)$, the average function $F(x) = \lim_{T\to\infty} 1/T \int_0^T f[A(x,t)]\,{\rm d}t$ should be invariant for any space shift, namely, $F(x) = F(x+a) = {\rm cons} \times \tan t)$. In this paper we use $f(A) = A_0(x,t)$. Therefore,

$$F(x) = \lim_{T\to\infty} \frac{1}{T} \int_0^T f[A_0(x,t)]\,{\rm d}t. \qquad (7)$$

This symmetry is confirmed by the approximately uniform distribution of $F(x)$ in Fig. 5(b) [for comparison, the highly heterogeneous distribution is shown in Fig. 5(a) for $L \le L_c$].

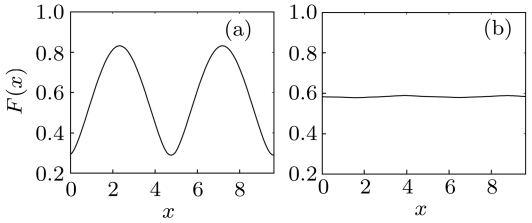


Fig. 5. Time-average amplitude distribution $F(x)$ before and after the L_c bifurcation (a) $L = 9.625$, (b) $L = 9.63$.

3.2. Instability to periodic alternations of the orientation of the Q2RW at L_f

In the size interval $L_f > L > L_e$ we have a stable running wave state, the Q2RW state. Though the dynamics of Eq. (1) is symmetric for both clockwise and anticlockwise orientations, the running wave state takes only one direction, according to its initial condition, and this is the so-called oriental symmetry ($S_{\rm O}$) breaking. After $L > L_f \approx 12.19$ this running wave state loses its stability via an intermittency of orientation alternations, shown in Fig. 6. In Fig. 6(a), we take $L = 12.18 < L_f$, and find well behaved running waves. In Fig. 6(b) L is slightly increased to $L = 12.2 > L_f$, some bursts appear during the running wave flow, and the running wave alternates its orientation after each burst, but the structure of the pattern between any two bursts in Fig. 6(b) is practically similar to Fig. 6(a). Therefore, in Fig. 6(b) no any particular orientation is prevailing for the state, and the oriental symmetry ($S_{\rm o}$) is recovered by the intermittency.

An interesting point is that the bursts in (b) appear periodically, and the variation of the amplitude is periodic too. Consequently, the motion of $A(x,t)$ is quasiperiodic with two frequencies. From $L < L_f$ to $L > L_f$, the motion keeps its quasiperiodicity with

two irreducible frequencies. However, the number of zero Lyapunov exponents increases from two to three [see Fig. 3(a)]. This is again the characteristic feature of spatiotemporal systems, and has no any counterpart in low dimensional temporal systems. The extra zero Lyapunov exponent for $L > L_f$ is due to the translational symmetry breaking at the intermittency, for which we will discuss below. The periodic bursts in Fig. 6 are sharply different from the chaotic bursts in Fig. 4. The reason for this difference can be intuitively understood. After the instability, a new mode appears and causes the periodic alternation of propagation orientation. In Fig. 4, the intermittency is due to the translation symmetry of Eq. (1) which forms a continuous group with infinite elements. The intermittency can freely choose its spatial distance for pattern shift, and the time intervals between these shifts must be irregular, thus the bursts should be random in both space and time. In Fig. 6, the intermittency is due to the orientational symmetry of Eq. (1), which forms a group with only two elements, clockwise and anticlockwise orientations, and periodicity of bursts can be easily organised between these two elements for both time and space.

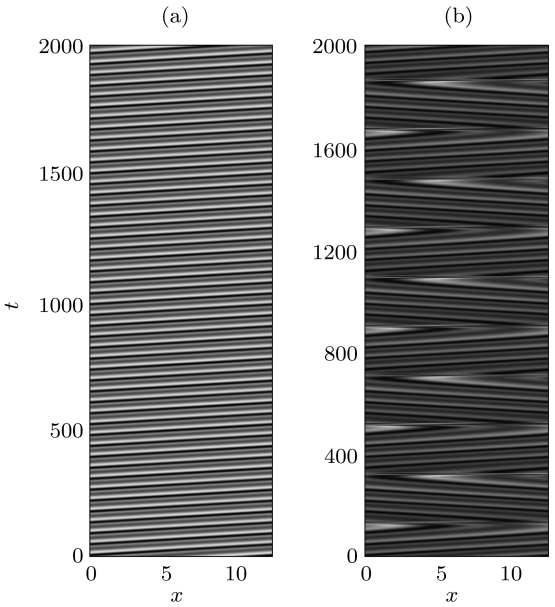


Fig. 6. Periodic alternation of propagation orientation around $L_f = 12.19$. (a) $L \approx 12.18 < L_f$, the pattern is a Q2RW state. (b) $L = 12.2$, periodic bursts alternate the orientation of the running waves. Between two neighbour bursts the pattern is similar to (a).

The intermittency at L_f recovers its statistical S_o symmetry as we discussed above. On the other hand, it destroys the statistical translational symmetry, which is shown in Fig. 7. In Fig. 7(a) we find uniform distribution of $F(x)$ for $L < L_f$, this is reasonable since all space points are equivalent to each other in the running wave state. In Fig. 7(b), the distribution becomes nonuniform, which indicates that different space points play different roles in the intermittent state, and the statistical S_T symmetry breaks. The apparent reason for this breaking is that the periodic orientation alternations in Fig. 6(b) appear at fixed space patterns. Different space points take different fixed related positions in the turning actions, and then they are no longer equivalent in the intermittent state.

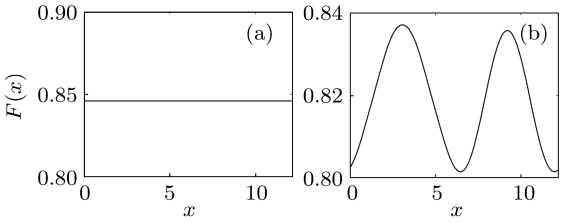


Fig. 7. (a), (b) The same as Fig. 5(a) and 5(b), respectively, with $L = 12.18$ (a) and $L = 12.2$ (b) being taken.

3.3. Intermittency from a 2-axis S_M symmetric Q2BW to a 1-axis S_M symmetric chaotic state

The 2-axis S_M symmetric state is stable in the region $L_m > L > L_k$. Reducing L to less than L_k, the Q2BW state becomes unstable, and a chaotic intermittency can be observed for L slightly smaller than L_k. In Fig. 8(a) we take $L = 17.8492 > L_k$, the motion is a regular Q2BW. Slightly reducing L to $L = 17.849 < L_k$, the motion in Fig. 8(b) manifests apparently an intermittent motion, for which the pattern in the laminar phase is almost the same as Fig. 8(a), while chaotic bursts break the laminar flow from time to time, and the time intervals between the bursts are randomly distributed.

The structure of the intermittency in Fig. 8(b) is strikingly different from that in Fig. 4(b). In the former case the S_M symmetry axes do not change their positions after each chaotic burst, but in the latter the axis makes random walks during bursts. This difference is due to the different natures of the S_M symmetry breakings in two cases. In Fig. 4, the S_M symmetry breaks completely during each burst, then the symmetry axis after the burst sensitively depends

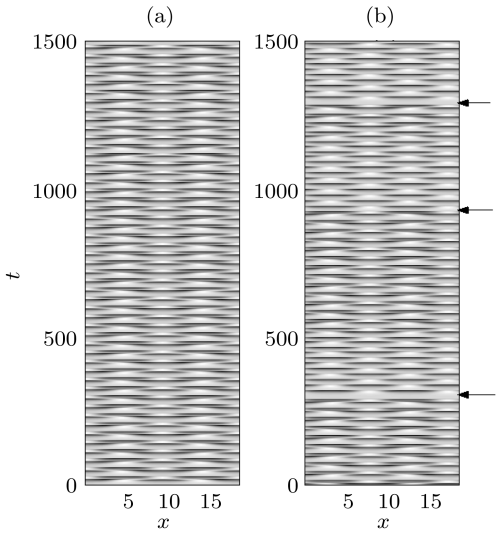


Fig. 8. Intermittency around $L_k \approx 17.8491$. (a) $L = 17.8492 > L_k$, the pattern is a Q2BW state with 2-axis $S_{\rm M}$ symmetry. (b) $L = 17.849 < L_k$, the pattern is similar to (a) in the laminar phase, and the directions of the two $S_{\rm M}$ axes are not changed by the chaotic bursts (the arrows indicate bursts). The largest LE in (b) is positive.

on any weak perturbation, and cannot be predicted. In Fig. 8, the 2-axis $S_{\rm M}$ symmetry [Fig. 9(a)] reduces to a smaller group of 1-axis $S_{\rm M}$ symmetry [Fig. 9(c)] at any burst of the intermittency, namely, during each burst only one symmetry axis ceases to play role, the other still keeps as an axis of $S_{\rm M}$ symmetry. In a given burst, the axis keeping in service is randomly chosen by the system motion among the two axes existing in the previous laminar phase period. And after each burst the remaining axis serves as a symmetry mark stone to help to rebuild another symmetry axis destroyed during the burst, and to recover the

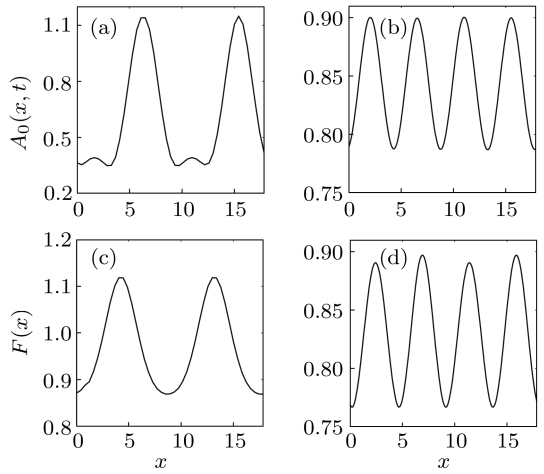


Fig. 9. (a), (b) $L = 17.8492$, amplitude distribution $A_0(x,t)$ at an arbitrary instant and time-average distribution of the amplitude $F(x)$, respectively. (c), (d) the same as (a) and (b), respectively, with $L = 17.849$. In (c) the time for the distribution is chosen at a chaotic burst.

entire 2-axis $S_{\rm M}$ symmetry with unchanged axes in the new laminar phase interval. Since the symmetry axes do not move, the statistical translational symmetry cannot be recovered in the intermittent state [see Figs. 9(b) and 9(d)], this is sharply different from the case of Fig. 5(b). It is noticed in Fig. 9(d) that the statistical $S_{\rm M}$ symmetry and $S_{\rm T}$ breaking are kept before and after the L_k bifurcation. To our knowledge, this is the first time the intermittency of type shown in Figs. 8 and 9 has discovered.

3.4. Transition from a quasiperiodic pattern to spatiotemporal chaos

In Fig. 3 we find that the last transition in our system to chaotic state occurs at $L_T = 18.746$, after which no any ordered state can be observed even for large L. Therefore, it is interesting to investigate how this final transition to turbulence takes place.

In Figs. 10(a) and 10(b) we amplify Figs. 3(a) and (4) for the largest LE λ_1. For $L < L_{T'}$, the motion is nonchaotic and the pattern is localised. In the previous section we knew that increasing L over L_m we observed a transition from the Q2BW state to the Q3BW state. At L_m, temporally, the system behaviour changes from two-frequency quasiperiodicity to three-frequency quasiperiodicity, and spatially, the state keeps its spatial order and localisation property after the bifurcation.

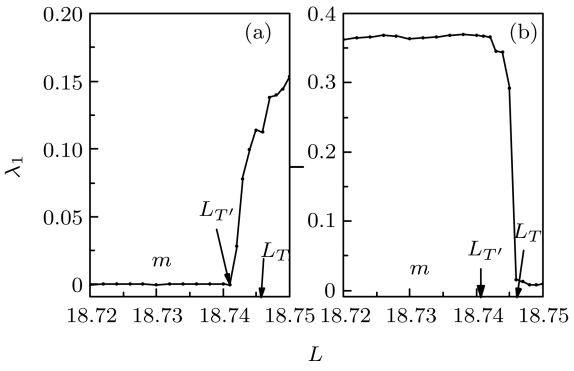


Fig. 10. (a) The largest LE λ_1 vs L around L_T. (b) The statistical quantity I vs L around L_T. At $L_{T'}$, λ_1 increases from zero to positive while $I(L)$ does not change much. However, at L_T, λ_1 has no characteristic change while $I(L)$ shows a discontinuous drop approximately to zero.

Further increasing L over $L_{T'} \approx 18.741$, the motion becomes chaotic with positive λ_1. However, comparing Figs. 10(a) and (b), we find that there still exists another bifurcation after $L_{T'}$ (i.e., at $L_T \approx 18.746$), which cannot be identified by the LE analysis in Fig. 10(a), but can be defined in Fig. 10(b) by the

transition of the order parameter $I(L) = F_{\max} - F_{\min}$ (where $F_{\max}$ and $F_{\min}$ are the maximum and minimum values of $F(x)$ against x) from positive to zero. In Fig. 11 we take $L_T > L = 18.744 > L_{T'}$, and investigate the spatiotemporal behaviour of the state. In the map of Fig. 11(c) the smooth circle in Fig. 11(b) breaks to scattering points, indicating a transition to chaos. However, the scattering points are still around the circle of Fig. 11(b), showing that chaos is not strong. The most interesting observation is that in Fig. 11(d) a clear 1-axis $S_{\rm M}$ symmetry exists. Further investigation shows that this $S_{\rm M}$ symmetry keeps for any instant. Consequently, in Fig. 11(e) the statistical distribution $F(x)$ has a clear localised structure with 4-axis $S_{\rm M}$ symmetry. Thus the state in the region $L_{T'} > L > L_T$ is a spatially well ordered and temporally chaotic state, and this spatial order can be clearly seen in Fig. 11(f). It is striking that a chaotic state (the largest LE $\lambda_1 \approx 0.1$) has such a nice pattern from global view.

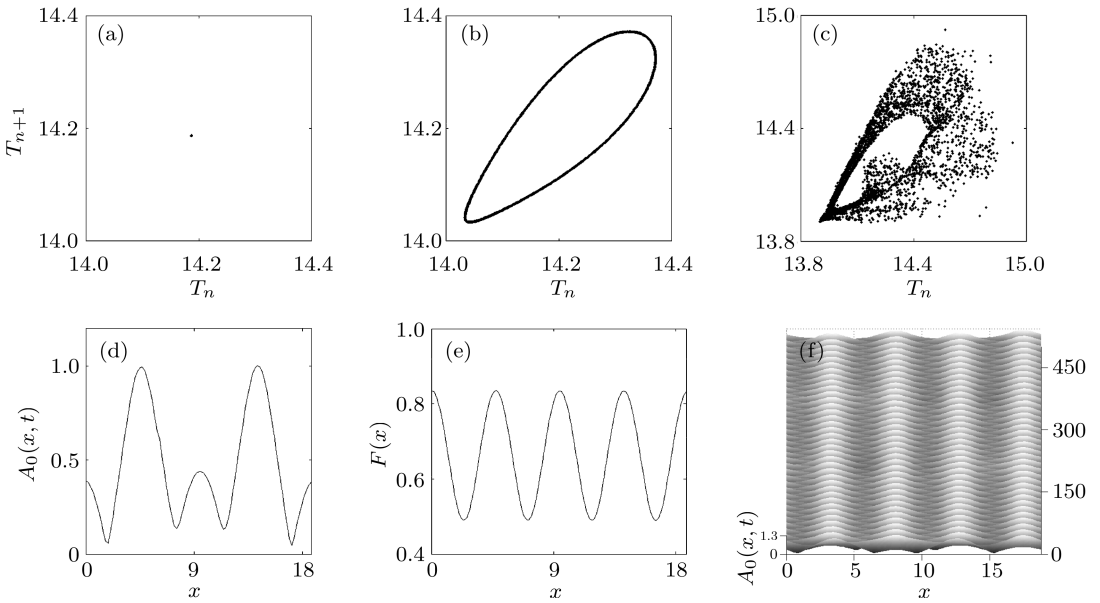


Fig. 11. (a), (b), (c) Amplitude maps $T_{n+1} - T_n$ for different L, where $T_n = t_{n+1} - t_n$ and t_n is determined by the nth crossing of the amplitude $A_0(x,t)$ with the value $A_0(x,t) = 0.3$ from up to down at an arbitrarily fixed space point. (a) $L = 18.72$. The map shows finite discrete points (we focus on a simple point in (a)). The amplitude varies periodically, and the motion is two-frequency quasiperiodic. (b) $L = 18.74$. The smooth circle shows two-frequency periodicity of the amplitude motion $A_0(x,t)$ and three-frequency quasiperiodicity of $A_0(x,t)$. (c)–(f) $L = 18.744$. (c) the same as (b) with L being changed. Scattering points around the smooth circle of (b) indicate a bifurcation from three-frequency quasiperiodicity to chaos. (d) $A_0(x,t)$ vs x at an arbitrary time instant, which keeps the 1-axis $S_{\rm M}$ symmetry. (e) Time-average amplitude distribution: $F(x)$ vs x. (f) The spatiotemporal pattern shows clearly spatial order for this temporally chaotic state.

From Figs. 10 and 11, we observe a clear road from quasiperiodic ordered pattern to a chaotic disordered state (spatiotemporal chaos). The road is from two-frequency quasiperiodic ordered (spatially) state to three-frequency quasiperiodic ordered state; to weak time chaotic and spatially ordered pattern; and finally to strong chaotic and spatially disordered turbulence. After $L > L_T$, all the instant $S_{\rm T}, S_{\rm M}$ and $S_{\rm O}$ symmetries break completely, while all the statistical $S_{\rm T}, S_{\rm M}$ and $S_{\rm O}$ symmetries are recovered fully. Further increasing L from $L > L_T$, the system will continuously go to the homogeneous turbulence, i.e., the defect turbulence, and no longer returns back to a regular state with spatial and temporal orders.

4. Conclusion

We have investigated a number of intermittencies new in the processes of a homogeneous periodic state to a high-dimensional defect turbulence state in the 1D CGLE by varying the system size only. A dy-

namical quantity—Lyapunov exponent, and a statistical quantity—the spatial distribution of time-average amplitude are used for the quantitative measurement of different pattern formations. We have discovered a number of interesting new states and new intermittencies. To our knowledge, it is the first time for us to observe the periodic alternation of propagation orientation in Fig. 6 in all intermittent states. The spatiotemporal intermittencies of types showed by Fig. 4 and Fig. 8 are also new for the CGLE system. Moreover, the transitions from two-frequency quasiperiodicity with 2-axis $S_{\rm M}$ spatial symmetry to three-frequency quasiperiodicity keeping spatial order and then to spatially ordered and temporally chaotic state; and finally to strong chaos with spatial disorder are significant and have not been reported before (to our knowledge).

While all the observations presented in this paper are based on numerical simulations, the mechanisms of some striking behaviours are intuitively (some are fully) understood, based on the symmetry analysis. The essential difference between the chaotic (in both time and space) intermittency in Fig. 4 and the periodic alternation of propagation orientation in Fig. 6 is explained by the difference of symmetry breaking of the continuous $S_{\rm T}$ symmetry with infinite elements and the discrete $S_{\rm O}$ symmetry with only two elements. And the difference between the random walk of the symmetry axis in Fig. 4 and the intermittency with spatially fixed $S_{\rm M}$ symmetry axes in Fig. 8 is due to the fact that the $S_{\rm M}$ symmetry is destroyed completely during the chaotic bursts in the former case while partial $S_{\rm M}$ symmetry (1-axis $S_{\rm M}$ symmetry) remains in the bursts of the latter case.

References

[1] Cross M C and Hohenburg P C 1993 *Rev. Mod. Phys.* **65** 851

[2] Kuramoto Y 1984 *Chemical Oscillations, Waves and Turbulence* (Tokyo: Springer)
Kuramoto Y and Koga S 1981 *Prog. Theor. Phys.* Suppl. **66** 1081

[3] Cross M and Hohenburg P 1994 *Science* **263** 1569
Ouyang Q and Flesselles J M 1996 *Nature* **379** 143
Egolf D and Greenside H 1994 *Nature* (London) **369** 129
Qu Z L, Weiss J N and Garfinkel A 2000 *Phys. Rev.* E **61** 727
Sun G Q, Jin Z, Liu Q X and Li L 2008 *Chin. Phys.* B **17** 3936
Ma J, Yi M, Li B W and Li Y L 2008 *Chin. Phys.* B **17** 2438

[4] Bohr T, Jensen M H, Paladin G and Vulpiani A 1998 *Dynamical Systems Approach to Turbulence* (Cambridge, England: Cambridge University Press)

[5] Coullet P, Gil L and Lega J 1989 *Phys. Rev. Lett.* **62** 1619
Shraiman B 1992 *Physica* D **57** 241

[6] Chate H and Manneville P 1987 *Phys. Rev. Lett.* **58** 112
Chate H, Pikovsky A and Rudzick O 1999 *Physica* D **131** 17

[7] Janiaud B, Pumir A, Bensimon D, Croquette V, Richter H and Kramer L 1992 *Physica* (Amsterdam) **55D** 269

[8] Chate H and Manneville P 1996 *Physica* A **224** 348

[9] Chate H 1994 *Nonlinearity* **7** 185
Cladis P E and Palffy-Muhoray P 1995 *Spatio-Temporal Pattern Formation in Nonequilibrium Complex Systems* (Reading MA: Addison Wesley) p33
Ma J, Gao C and Tan L Y 2007 *Chin. Phys.* **16** 1327

[10] Montagne R, Hernandez-Garcia E and San Miguel M 1996 *Phys. Rev. Lett.* **77** 267
Montagne R, Hernández-García E, Amengual A and San Miguel M 1997 *Phys. Rev.* E **56** 151

[11] Torcini A 1996 *Phys. Rev. Lett.* **77** 1047
Torcini A, Frauenkron H and Grassberger P 1997 *Phys. Rev.* E **55** 5073

[12] van Saarloos W and Hohenberg P C 1992 *Physica* (Amsterdam) **56D** 303
van Saarloos W and Hohenberg P C 1993 *Physica* (Amsterdam) **69D** 209 (Errata)

[13] van Hecke M 1998 *Phys. Rev. Lett.* **80** 1896

[14] Chaté H 1995 *Physica* (Amsterdam) **86D** 238

[15] Popp S, Stiller O, Aranson I, Weber A and Kramer L 1993 *Phys. Rev. Lett.* **70** 3880

[16] Torcini A 1996 *Phys. Rev. Lett.* **77** 1047

[17] Aston P J and Laing C R 2000 *Physica* D **135** 79
Fujisaka H, Ouchi K, Hata H, Masaoka B and Miyazaki S 1998 *Physica* D **114** 237

[18] Carolina B, Igor S A and Hugues C 2003 *Phys. Rev. Lett.* **90** 068301

[19] Abarzhi S I, Desjardins O, Nepomnyashchy A and Pitsch H 2007 *Phys. Rev.* E **75** 046208

[20] Zhou Q, Chen Z Q and Yuan Z Z 2007 *Chin. Phys.* **16** 1616

[21] Benjamin T B and Feir J E 1967 *J. Fluid Mech.* **27** 417

[22] Hu B and Rudnick J 1982 *Phys. Rev. Lett.* **48** 1645

[23] Heagy J F, Platt N and Hammel S M 1994 *Phys. Rev.* E **49** 1140